Journal of Magnetics 6(3), 94-100 (2001)

Magnetic Behaviors of Isolated Fe-Co-Ni Nanoparticles in a Random Arrangement

Choong Jin Yang*, Kyung Soo Kim[1] and Jianmin Wu[2]

Research Institute of Industrial Science & Technology, Electromagnetic Materials, Lab., P.O. Box 135, Pohang 790-600, Korea
[1]Dept. of Physics, Yeungnam University, Kyongsan 712-749, Korea
[2]Dept. of Functional Materials, Central Iron & Steel Research Institute

(Received 2 March 2001)

Fe-Co-Ni particles with an average size of 45 and 135 nm are characterized in terms of magnetic phase transformation and magnetic properties at room temperature. BCC structure of Fe-Co-Ni spherical particles can be synthesized from Fe-Co-Ni-Al-Cu precursor films by heating at 600~800°C for the phase separation of Fe-Co rich Fe-Co-Ni particles, followed by a post heating at 600°C for 5 hours. The average size of nanoparticles was directly determined by the thickness of precursor films. Exchange interactive hysteresis was observed for the nano-composite (Fe-Co-Ni)+(Fe-Ni-Al) films resulting from the short exchange interface between ferromagnetic Fe-Co-Ni particles surrounded by almost papramagnetic Ni-Al-Fe matrix. Arraying the isolated Fe-Co-Ni nanoparticles in a random arrangement on Al_2O_3 substrate the particle assembly showed a behavior of dipole interactive ferromagnetic clusters depending on their volume and inter-particle distance.

Key words : nanoparticle, Fe-Co-Ni ferromagnetic, spinodal decomposition, exchange coupling

1. Introduction

The magnetic properties of fine ferromagnetic particles with diameters typically about 10 nm are governed by two characteristics, the single-domain magnetic structure and an enhanced coercivity. The former occurs because the size of the system is smaller than the exchange correlation length and latter is a consequence of the reduced crystal symmetry near the surface originating from the finite size and possible existence of surface disorder [1]. The magnetic behavior of an assembly of noninteracting fine particles with uniaxial anisotropy is understood on the basis of Néel's argument [2] that led to the concept of superparamagnetism [3]. The exploitation of this phenomenon in the determination of the particle size distribution has been the subject of intensive experimental and theoretical work over the last decade [4].

Magnetic granular alloys consisting of a distribution of fine magnetic particles embedded in a nonmagnetic metallic matrix have generated great interest due to their technological applications and their new challenging magnetic and transport properties [5, 6]. Since the granular magnetic solids consisting of heterogeneous alloys of magnetic material in a nonmagnetic host would determine the status of intergranular exchange effect while dipolar interactions are intrinsic in dispersions of fine magnetic particles [7]. The Wolfarth model predicts that the remanence-saturation magnetization ratio is 0.5 for a random distribution of noninteracting uniaxial single domain particles with coherent rotation of the total magnetization. However, deviations from this ideal value are observed in real systems due to interparticle interactions and textured growth. The effect of dipolar interactions or exchange interaction on M_r/M_s is strongly dependent on both their strength and local distribution. Also they may either enhance or reduce remanence [8-10].

Ferromagnetic nanoparticles has been the subject of considerable experimental work in recent years. Ball milling synthesis routes were employed to prepare Fe [11] and Ni [12] nanoparticles and the magnetic properties was characterized by Mössbauer spectroscopy, and magnetoelastic behavior was evaluated, respectively. Magnetic nano-elements of Ni-Fe [13] and Co-Fe [14] systems have been fabricated by e-beam lithography and lift-off patterning, and their switching behavior and interactions between the nano arrays were studied. Recent study on magnetic properties of NiFe particles synthesized by a mechanochemical process was also reported [15]. In this work we employed multi-step heat treatment process to prepare the ferromagnetic nanoparticles, which involves evaporation of nano-thick multi-phased precursor (Fe-Co) + (Ni-Al) + (Fe-Ni) films followed by prolonged heating for the formation of isolated Fe-Co-Ni nanoparticles in a random arrangement. The magnetic properties were evaluated in terms of particle size as a function of precipitation process temperature.

*Tel: +82-54-279-6331, e-mail: cjyang@rist.re.kr

2. Synthesis of Nanoparticles and their Magnetic Characterization

Fe-Co-Ni-Al-Cu films 45 and 135 nm thick, respectively, were RF/DC magnetron sputtered onto Al_2O_3 substrate using a 50.7 wt.% Fe-23.5Co-14.4Ni-8.4Al-3.0Cu target. The deposition was performed at room temperature under Ar pressure of 10×10^{-6} Torr at a deposition rate of 170 Å/min using a sputtering energy of 200 W/cm^3. Al was added to induce the formation of Ni-Al paramagnetic phase during the first step of heat treatment, and Cu was added to increase the (Fe-Co)-(Ni-Al) immiscibility so as to spur the granular precipitation of the Fe-Co rich phase from Ni-Al rich matrix during the heat treatment [16]. The deposited films were heat treated following by two-step; first heating at 600~800 °C for 20~60 min. so as to increase the portion of Fe-Co-Ni phase, and then second heating was followed at 600 °C for 5 hours so as to evaporate the volatile Al from Ni-Al rich Fe-Ni-Al phase and recombine the Ni into Fe-Co-Ni into a spherical shape. During the first heating film samples were sealed in a quartz tube filled with Ar gas at about 2 atm. pressure. However, the second heating was carried out in vacuum. After the final heat treatment samples were cooled in the identical furnace. An external magnetic field of 4.5 kOe was applied in-plane direction during the first heating in order to align the ferromagnetic phase, which was later precipitated from the paramagnetic matrix.

After completion of the second heating, nanoparticles of Fe-Co-Ni were formed on the Al_2O_3 substrate in a random array of isolated particles. Magnetic measurements were made along both in-plane and perpendicular directions. However, the nanoparticles on the Al_2O_3 substrate exhibited a negligible magnetization along the perpendicular direction. Accordingly, discussions were focused on the case of in-plane measurements. Every data point in this study is the average value of three measurements of which hundreds of measurements were made. A vibrating sample magnetometer was used for the magnetic characterization, and high resolution TEM and SEM (both are field effect microscopes) were used to identify the nanoparticles.

3. Results and Discussion

3.1. Phase transformation and the synthesis of Fe-Co-Ni nanoparticles

Fig. 1 shows x-ray diffractions of magnetic phases formed during the first step heating of precursor Fe-Co-Ni-Al-Cu films, and the magnetic phases in the target used for the film deposition. The target material consisted of ferromagnetic Fe-Co rich acicular particles embedded in Ni-Al rich matrix. Both the Fe-Co and Ni-Al was confirmed to be of BCC structure. As deposited films before heating also indicated the formation of (110)Fe-Co and (200)Ni-Al together with the presence of Fe_3O_4. However, after the first step heating at 650, 800 and 850 °C for 20 min., the films

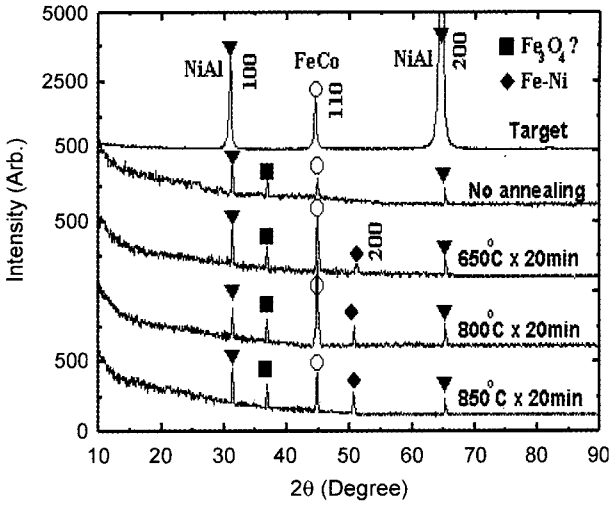

Fig. 1. X-ray diffraction patterns of films after spinodal decomposition during the first step heating at various temperature for the Fe-Co-Ni-Al-Cu precursor films, and target used.

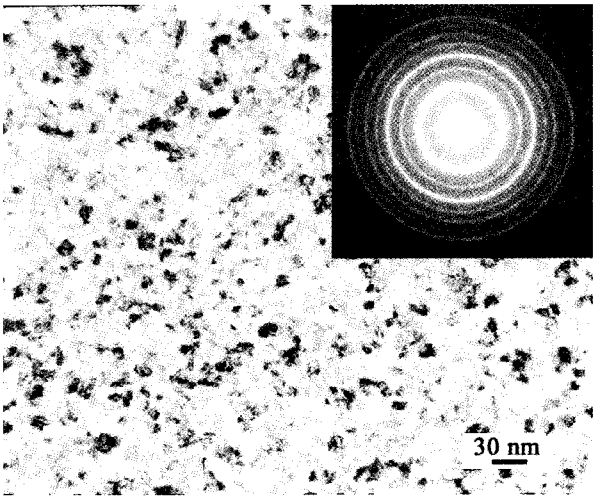

Fig. 2. High resolution TEM micrograph of the sputtered films at room temperature. Fe-Co-Ni nanoparticles are seen to form embedded in the matrix of mother alloy composition.

commonly indicate the formation of Fe-Ni, which become active with increasing the heating temperature. Instead the paramagnetic Ni-Al phase tends to decrease with the increase of heating temperature, which is indicated by the diminished peaks of the both (100) and (200) planes. More detailed microstructure was identified by high resolution TEM technique. Fig. 2 shows the Fe-Co-Ni rich particles less than 10 nm size embedded in the matrix of mother alloy composition, which has been already formed after the deposition at room temperature. Highly magnified structure in Fig. 3 shows the nanoparticles of Fe-Co rich Fe-Co-Ni composition developed in (110) direction as shown in the inset. An accurate energy dispersion analysis gave the composition of particles as Fe; 42 wt. %, Co; 23.5 wt. %, Ni; 12.5 wt. %, Al; 5.3 wt. %, and O; 4.9 wt. %, and the rest was Cu. Since Cu grid was used for the examination TEM

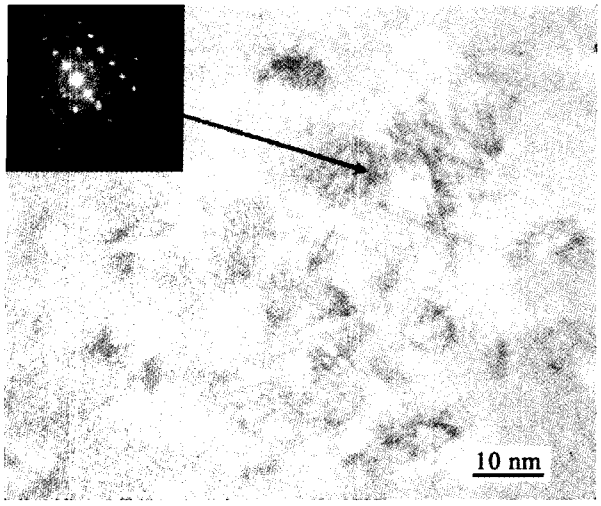

Fig. 3. Magnified high resolution TEM micrograph showing the nanoparticles of Fe-Co-Ni phase in the amorphous matrix.

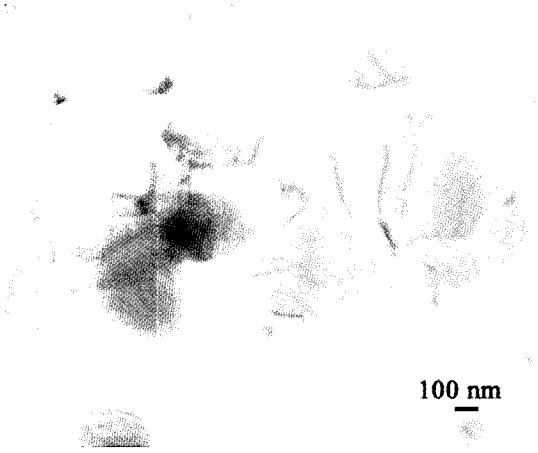

Fig. 4. Fe-Co-Ni rich particles formed during the spinodal-like decomposition at 800 °C for 20 min. The black circular area corresponds to the Fe-Co-Ni rich particles.

microscopy and EDX, the Cu content was measured to be relatively high. Taking into account the results of both the x-ray and TEM analyses, the microstructure of as-deposited films is seems to consist of Fe-Co rich Fe-Co-Ni particles embedded in Ni-Al rich Ni-Al-Cu amorphous matrix.

After the first heating at 650~800 °C for 20~40 min., the basic structure of the precursor films was not changed. However, the previous Fe-Co-Ni particles were confirmed to have grown to quite a measurable size as shown in Fig. 4 where the particles appear as dark circles and needles. Furthermore the Al content was measured to be 3.5~4.0 wt. % which was reduced by 24.5~34%. At the same time Ni content was found to increase approximately 124%. It is assumed, therefore, that the phase separation of Fe-Co rich Fe-Co-Ni and Fe-Ni rich Fe-Ni-Al phase took place completely on the basis of spinodal-like decomposition [17]. However, it is not quite sure whether the process was really spinodal decomposition or not at the moment. Immediately after this phase separation, however, volatile Al seems to

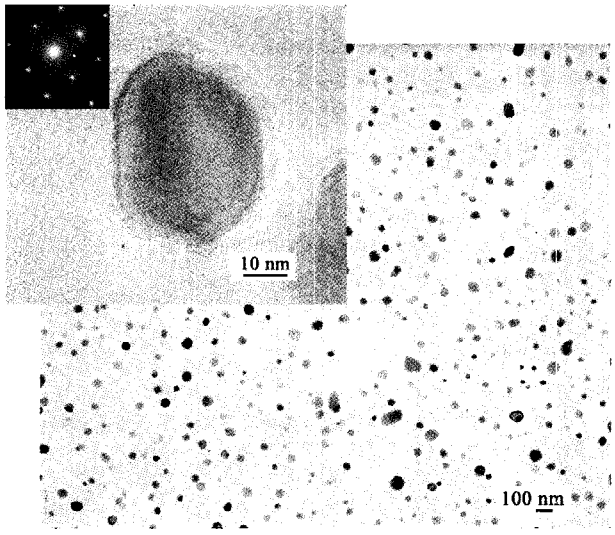

Fig. 5. Fe-Co-Ni nanoparticles isolated in a random arrangement after the first step heating at 800 °C for 20 min, and followed by 600 °C for 5 hours heating. The inset indicates the single particle grown in [001] direction perpendicular to the film plane.

evaporate and Ni tends to diffuse into neighboring Fe-Co rich Fe-Co-Ni particles resulting in the growth of existing Fe-Co-Ni particles as was already suggested in Fig. 1 already. During this process some absorption of oxygen may be unavoidable due to the large surface of nanoparticles. Naturally the formation Fe_3O_4 was detected.

During the second step of prolonged heating at 600 °C for 5 hours, the evaporation of Al was completed, and the growth of the existing Fe-Co-Ni particles proceeded into easy magnetization direction as shown in Fig. 5. The inset is a magnified nanoparticle indicating the preferred orientation [001] in a direction perpendicular to the substrate plane. The photo was taken from a sample prepared on carbon film deposited onto a Cu grid. An accurate EDX examination gave the average composition of nanoparticles as Fe; 37.0 wt. %, Co; 21.8 wt. %, Ni; 20.5 wt. %, Al; 0.35 wt. %, and O; 2.52 wt. %. The rest was Cu content which was from grid materials. However, the Cu content measured from particles on Al_2O_3 substrate was less than 1.0 wt. %.

3.2. Magnetic properties of Fe-Co-Ni nanoparticles embedded in Fe-Ni-Al matrix after Spinodal-like decomposition

As discussed already, the ferromagnetic Fe-Co rich Fe-Co-Ni nanoparticles were precipitated by spinodal-like decomposition of Fe-Co-Ni-Al-Cu. In addition to the ferromagnetic particles were found to be surrounded by a paramagnetic Ni-Al rich, more specifically in this study, very weak ferromagnetic Ni-Al rich Fe-Ni-Al matrix. Fig. 6 shows magnified hysteresis curves of the composite films 45 and 135 nm thick after the first step of heating. The films were heated at 650 °C for 20 min. During the heating an external field of 4.5 kOe was applied in-plane direction

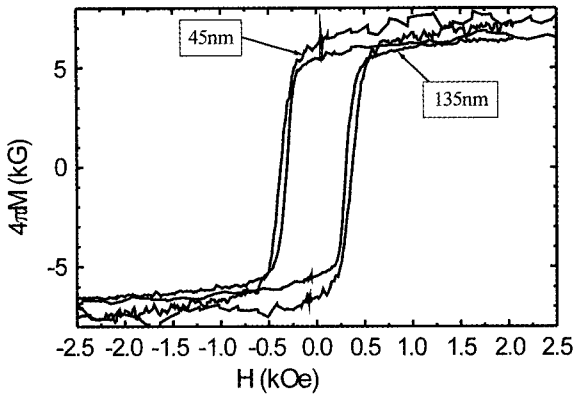

Fig. 6. The typical hysteresis curves of the films after the first step heating at 650 °C for 20 min at 4.5 kOe of magnetic filed for the spinodal-like decomposition of different thickness of film.

of the specimen. The films, 135 nm thick of nano-composite Fe-Co-Ni and Fe-Ni-Al, indicate the typical ferromagnetic behavior, which means that the hysteresis was obtained by the demagnetization process of non-interacting Fe-Co-Ni nanoparticles. For this case, Fe-Co-Ni particles were surrounded by thick layers of weak ferromagnetic Fe-Ni-Al phase. Therefore, the Fe-Co-Ni particles behaved like well-isolated particles. However, the spinodal-like decomposition in films 45 nm thick would take place in a short range of compositional fluctuation, which leads to a smaller size of Fe-Co-Ni particles and shorter inter-particles distance. In magnetic granular alloys consisting of a random distribution of fine magnetic particles embedded in a non-magnetic metallic matrix, inter-particle interactions are dipolar and exchange in nature [7, 9]. The hysteresis of 45 nm thick films in Fig. 6 indicates the exchange interaction suggested by the very coercive magnetic reversal shown up to a field of 2.0 kOe. This suspended magnetization reversal is prominent compared with that of 135 nm thick films. The exchange interaction between nanoparticles is also suggested by the serration along the magnetization curve far to the saturation field which is not observed in 135 nm thick

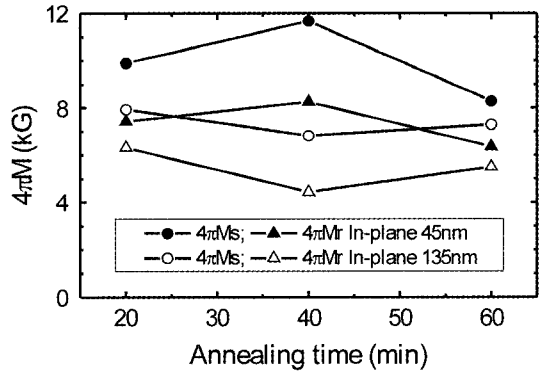

Fig. 7. The variations of $4\pi M_r$ and $4\pi M_s$ of the films after the first step heating at 650 °C for various time. (M_s was the saturated value measured at the maximum magnetic filed of 20 kOe.)

films. Those behaviors were also true for the nano-composite films heated for 40 and 60 min, respectively. Consequently superior saturation and remanent magnetization of 45 nm thick films to the 135 nm thick films were noticable as shown in Fig. 7. However, one question still remaines to be solved. The coercivity shown in Fig. 6 for 45 nm thick films suggested a higher value than that of 135 nm thick films. If those ferromagnetic Fe-Co rich Fe-Co-Ni particles embedded in paramagnetic Ni-Al-Fe matrix were supposed to form, finer particles of ferromagnetic phase should exhibit a higher coercivity value. At present study, however, the spinodal-like process is not clarified exactly, and accordingly the ferromagnetic particles would not be a completely isolated particle after the first heat treatment. Consequently, the hysteresis behavior shown in Fig. 6 might not be typical.

The variation of magnetic properties in Fig. 7 also can be rationalized in a different point of view. During the spinodal-like decomposition at 650 °C for 20, 40 and 60 min, respectively, the time for a complete phase separation would not be the same. The phase separation process of Fe-Co-Ni particles for the films 135 nm thick might not be enough compared with that of films 45 nm thick. Accordingly the 135 nm thick films contain less ferromagnetic particles than in the 45 nm thick films, which result in low values of $4\pi M_s$ and $4\pi M_r$ as well. This explanation suggests a compositional difference of Fe-Co-Ni particles synthesized in two different thickness of precursor films, and this was confirmed in fact.

3.3. Magnetic behaviors of isolated Fe-Co-Ni nanoparticles on non-magnetic Al_2O_3 substrate in a random arrangement

Following the second step heating at 600 °C for 5 hours, complete isolation of Fe-Co-Ni nanoparticles was possible as shown in Fig. 5. Taking into account the prolonged heating treatment for the arrangement of well-isolated Fe-Co-Ni particles, most of the particles of B.C.C. are believed to grow with their cubic axes parallel to the plane direction. During this arrangement the vaporization of Al and recombination of Ni into Fe-Co-Ni particles were taking place, and the new crystals must settle down with their least energy of crystallization. Accordingly their <001> crystallographic axes are at 90° with respect to the substrate surface as shown in the inset of Fig. 5 indicating the nano diffraction pattern of [001] B.C.C. crystal.

In order to discuss the magnetic behaviors of Fe-Co-Ni nanoparticles, the final magnetic properties of completely isolated particles in a random arrangement were characterized as a function of phase separation temperature during the spinodal-like decomposition. The phase separation of ferromagnetic Fe-Co-Ni particles from almost paramagnetic Ni-Al-Fe matrix basically dependent upon this temperature. The size and distribution of nanoparticles should be organized during this treatment. More importantly, as mentioned

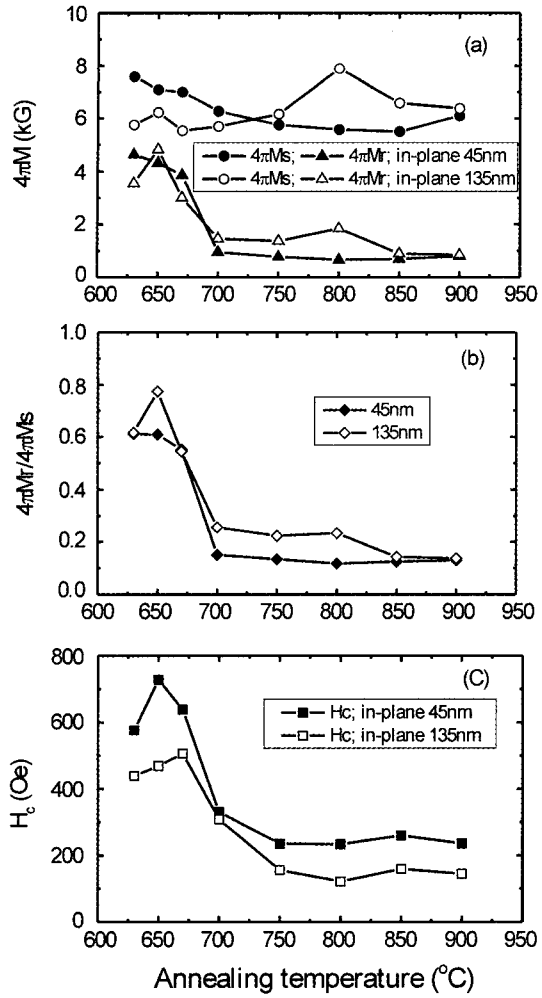

Fig. 8. The variation of magnetic properties of Fe-Co-Ni nanopatrticles of 45 and 135 nm size synthesized after the final treatment as a function of first step heating temperature.

already the obtained size of nanoparticles formed on Al_2O_3 substrate were found to be almost identical or slightly larger than the thickness of precursor films. Fig. 8(a), (b) and (c) show the variations of $4\pi M_r$ and $4\pi M_s$, $4\pi M_r/4\pi M_s$ ratio, and H_c, respectively, as a function of temperature during the first step heating which was carried out for 20 min at the indicated temperatures, and followed by the second step heating at 600° for 5 hours for all the samples. First of all, the variations of magnetic properties for the particles of 45 and 135 nm as a function of precipitation temperature show almost common behaviors. Both of the particles of 45 and 135 nm exhibit the $4\pi M_s$ values about 6~7 kG regardless of the treatment temperature as shown in Fig. 8(a). However, $4\pi M_r$ values behave quite differently. The remanence values of the nanoparticles precipitated at 630~670 °C during spinodal-like decomposition and then heated at 600 °C for 5 hours tend to maintain the previous properties of precursor films ranging around 3.5~4.5 kG. These values are close to those shown in Fig. 7 illustrating the properties of precursor films composing of Fe-Co-Ni and Ni-Al-Fe phases. However, the nanoparticles which precipitated at a temperature higher than 700 °C show very low values less than 2 kG after the final treatment. $4\pi M_r/4\pi M_s$ ratios are plotted in Fig. 8(b), and the variation shows an almost identical trend to that of remanence for both size particles.

Two approaches are made to explain the magnetic behaviors mentioned above. One is the compositional difference in the ferromagnetic particles precipitated during the spinodal-like decomposition. The other is exchange interaction between randomly arrayed nanoparticles. The composition of target used in this study was 50.7 wt.% Fe-23.5Co-14.4Ni-8.4Al-3.0Cu which was almost identical to that of Alnico 5 permanent magnet. For this Alnico 5 magnet the optimized spinodal decomposition has been recommended to occur at 775 °C for a well defined ferromagnetic Fe-Co rich and very paramagnetic Ni-Al rich phase [18]. When the both phases are well defined, the composition of Fe rich particle is similar to Fe_2Co with some Ni, and the other is NiAl with small amount of Fe. In this study we confirmed the composition of precipitated ferromagnetic particles to have Fe;42 wt%, Co;23.5 wt%, and of Ni;12.5 wt%, Al;5.3 wt %, respectively. Although each phase must contain three components at the same time, it was very hard to distinguish each component in each magnetic phase. Only we confirmed that the Fe-Co rich phase is close to Fe_2Co. If the spinodal-like decomposition is assumed to occur at a lower temperature, *i.e.*, lower than 700 °C as shown in Fig. 8, we can guess that the ferromagnetic Fe rich Fe-Co-Ni particles should have less content of Fe-Co. If this happens the magnetic properties of those particles naturally exhibit a less hard magnetic character. Accordingly, those particles show a higher remanence value due to their soft magnetic characteristics. Therefore a higher reduced remanence ratio (M_r/M_s) can be seen in Fig. 8(b) in the low decomposition temperature range.

Another discussion is remained to explain why the reduced remanence ratios are much smaller than the Wohlfarths prediction M_r/M_s=0.5 for every samples of nanoparticles, and why the reduced remanence and coercivity drop right after the higher spinodal-like decomposition temperature than 700 °C as shown in Fig. (b) and (c). According to Stoner-Wohlfarth [19] the coercivity of an aligned assembly of identical non-interacting infinitely dilute single domain particles with uniaxial shape anoisotropy is

$$H_c = (D_z\text{-}D_x)M_s$$

i.e., the coercivity is proportional to the saturation magnetization and the difference of demagnetization factors (D_z, D_x). Since the coercivity depends on the presence of demagnetization fields it is clear that the nanoparticles interactions cannot be neglected.

The previous classic reports [2, 20] suggested that the effects of nanoparticle interactions on the coercivity are best described by the relation

$$H_c(p) = H_c(0)(1\text{-}p)$$

where $H_c(p)$ is the coercivity for a nanoparticle packing fraction "p" and $H_c(0)$ is the coercivity for a packing fraction zero. Thus if the effects of nanoparticle interactions are involved, the coercivity of a fully aligned array of single domain particles with uniaxial shape anisotropy is

$$H_c = (1\text{-p})\, DM_s$$

In the present study, however, the nanopatrticles of spherical shape give the demagnetization factor $D=D_z=D_y=D_x=1/3$. Accordingly, the coercivity of present nanoparticles can be denoted as

$$H_c = 0.33(1\text{-p})M_s$$

It is assumed, therefore, that H_c will behave like that of saturation magnetization, M_s. Since the composition of nanoparticles synthesized via present process was determined basically from the final stage of spinodal-like decomposition, the Fe-Co-Ni nanoparticles decomposed at each different temperature will have different average compositions, and therefore different M_r. Namely the M_r at each temperature varies with an identical trend to the M_r/M_s ratios shown in Fig. 8(b). For a fixed volume fraction of Fe-Co-Ni nanoparticles, for instance, with a supposed "p" of 0.4 using the measured M_s of 6 kG, the estimated H_c is obtained to be 792 Oe, which is quite a high value compared with measured H_c in Fig. 8(c). Accordingly one cannot exclude the effect of nanoparticles interaction.

In fact the loss of remanence and coercivty was reported frequently which are attributed to macroscopic quantum tunneling [9], or to dipole interaction [21], or underestimated M_s [9]. All previous work reported reduced remanence which was much smaller than 0.5. Fig. 5 shows the isolated nanoparticles in a random arrangement, and the average inter-particle distance can be seen to be about 100 nm. In this case the attribution from quantum tunneling should be excluded. However, dipole interaction was always reported responsible for the reduced remanence and coercivty as well [9, 21] which were proved experimentally and by Monte Carlo simulations as well.

Also those elaborated simulations showed that the increase in particle concentration enhances coercivity. Physically the shorter inter-particle distance corresponds to exchange length within the nanoscale of 10~20 nm. In this study the inter-particle distance of nanoparticles synthesized from 135 nm thick films was found to be longer, and the volume fraction of remaining nanoparticles was also lower than those particles made from 45 nm thick films. Accordingly, the coercivities of smaller size particles were measured to be higher than those of 135 nm particles. At the same time the intrinsically lower value of H_c for the 135 nm particles should be also responsible, because the spinodal-like decomposition in a thick film may take longer time for a complete phase separation than in a thin film, which results in less hard magnetic properties shown in Fig. 8. Fig. 9 shows the hysteresis behavior of Fe-Co-Ni particles

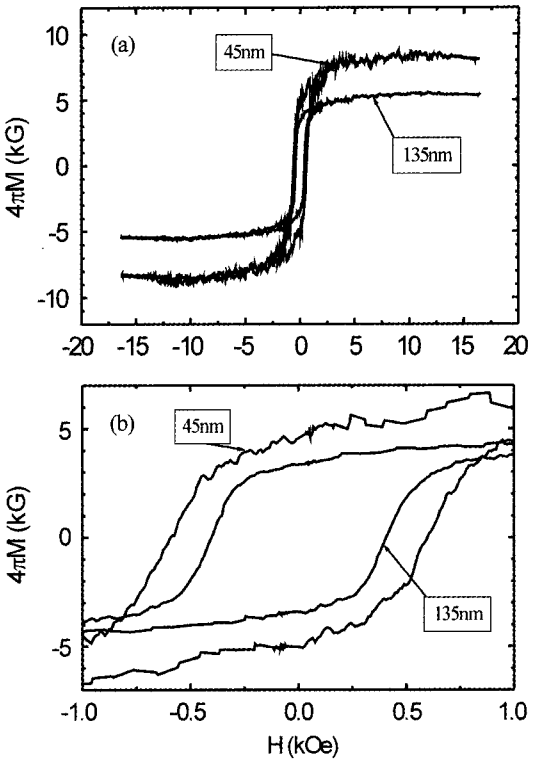

Fig. 9. The typical hysteresis curves of 45 and 135 nm size nanaoparticles in a random arrangement on Al_2O_3 substrate after the final heat treatment.

with the size of 45 and 135 nm which were synthesized following the identical procedure with the sample shown in Fig. 8. Both the remanence and coercivity for the particles 45 nm indicate the existing interaction between nanoparticles. Besides the serrated magnetization process shown along the hysteresis curve suggests the possible interaction which is not shown, however, for the 135 nm particles.

4. Conclusion

Fe-Co-Ni particles with an average size of 45 and 135 nm are characterized in terms of magnetic phase transformation and magnetic properties at room temperature. BCC structure of Fe-Co-Ni particles were able to be synthesized from Fe-Co-Ni-Al-Cu precursor films after heating at 600~800 °C for the phase separation of Fe-Co rich Fe-Co-Ni particles followed by a post heating at 600 °C for 5 hours. Both the Fe-Co-Ni nanoparticles of 45 and 135 nm in a random arrangement suggested a dipole interaction between the isolated nanoparticle. The loss of remanence and coercivity was prominent for the nanoparticles in a random arrangement due to their exchange interactions. A higher volume fraction, therefore, closer inter-particle distance for the particles assemble of 45 nm indicated a prominent exchange interaction. However, the magnetic properties of nanoparticles assembly are basically determined by the characteristics of previously decomposed ferromagnetic Fe-Co-Ni particle during phase separation.

Acknowledgement

This work was financially supported by The Korean Ministry of Science & Technology under Frontier Nanotechnology Project contract No. 2000D030, and Nano Technology 1999E006. This work was partially supported also by the Research Center for Advanced Magnetic Materials under contract No. 2000D004.

References

[1] J. L. Dorman, D. Fiorani and E. Tronc, Adv. Chem. Phys. **98**, 283 (1997).
[2] L. Néel, C. R. Hebd, Seances Acad. Sci. **228** (1949) 664; Ann. Geophys (C.N.R.S) **5**, 99 (1949).
[3] C. P. Bean and J. D. Livingston, J. Appl. Phys. **30**, 120 (1959).
[4] Magnetic Properties of Fine Particles, ed. by J. L. Dormann and D. Fiorani (North-Holland, Amsterdam, 1992).
[5] A. E. Berkowitz, J. R. Mitchell, M. J. Carey and G. Thomas, Phy. Rev. Lett. **68**, 3745 (1992), and ibid. **68**, 3749 (1992).
[6] R. W. Chantrell, in Science & Technology of Nanostructured Magnetic Materials ed. by G. C. Hadjipanayis and G. A. Prinz (Plenum, New York, 1991), NATO Advanced Series **259**.
[7] X. Battle, V. Franco, A. Labata and K. O'Grady, J. Appl. Phys. **88**(3), 1578 (2000).
[8] D. Kechrakos and K. Trohudou, Phys. Rev. B **58**, 169 (1998).
[9] M. El-Hilo, R. W. Chantrell and O'Grady, J. Appl. Phys. **84**, 5114 (1998).
[10] W. Luo, S. R. Nagel, T. F. Rosenbaum and R. E. Rosenwieg, Phys. Rev. Lett. **67**, 2721 (1991).
[11] L. D. Bianco, A. Hernando and E. Bonetti, J. of Magn. & Magn. Mater. **171-181**, 939 (1998).
[12] E. Botteni, E. G. Campari, L. Pasquini and E. Sampaolesi, J. Appl. Phys. **84**(8), 4219 (1998).
[13] K. J. Kirk, J. N. Chapman, S. McVitie and P. R. Aitchson, J. Appl. Phys. **87**(9), 5105 (2000).
[14] C. E. Moreau, J. A. Caballero, R. Loloee and N. O. Birge, J. Appl. Phys. **87**(9), 6316 (2000).
[15] X. Y. Quin, J. S. Lee and J. G. Kim, J. Appl. Phys. **86**(4), 2146 (1999).
[16] R. A. McCurrie, in *Ferromagnetic Materials*, ed. by E. P. Wohlfarth, (North-Holand, Amsterdam, 1982), Vol. **3**, pp. 112.
[17] ibid, pp. 147.
[18] De Vos, in Alnico Permanent Magnet Alloys, ed. by A.E. Berkowitz and E. Kneller, (Academic Press, New York, 1969), pp.473.
[19] E. C. Stoner and E. P. Wohlfarth, Philos. Trans. R. Soc. London, Ser. A **240**, 599 (1948).
[20] H. Zijlstra, Z. Angew. Phys. **21**, 251 (1962).
[21] S. Mahmood and I. Abu-Aljarayesh, J. Magn. Magn. Mater. **118**, 193 (1993).